

This discussion paper is/has been under review for the journal *Climate of the Past* (CP).
Please refer to the corresponding final paper in CP if available.

An assessment of climate state reconstructions

S. Dubinkina and
H. Goosse

An assessment of climate state reconstructions obtained using particle filtering methods

S. Dubinkina and H. Goosse

Earth and Life Institute, Georges Lemaître Centre for Earth and Climate Research, Université catholique de Louvain, P.O. Box L4.03.07, 1348 Louvain-la-Neuve, Belgium

Received: 12 December 2012 – Accepted: 18 December 2012 – Published: 3 January 2013

Correspondence to: S. Dubinkina (svetlana.dubinkina@uclouvain.be)

Published by Copernicus Publications on behalf of the European Geosciences Union.

Title Page

Abstract

Introduction

Conclusions

References

Tables

Figures

⏪

⏩

◀

▶

Back

Close

Full Screen / Esc

Printer-friendly Version

Interactive Discussion

Abstract

In an idealized framework, we assess reconstructions of the climate state of the Southern Hemisphere during the past 150 yr using the climate model of intermediate complexity LOVECLIM and three data-assimilation methods: a nudging, a particle filter with sequential importance resampling, and an extremely efficient particle filter. The methods constrain the model by pseudo-observations of surface air temperature anomalies obtained from a twin experiment using the same model but different initial conditions. The net of the pseudo-observations is chosen to be either dense (when the pseudo-observations are given at every grid cell of the model) or sparse (when the pseudo-observations are given at the same locations as the dataset of instrumental surface temperature records HADCRUT3). All three data-assimilation methods provide with good estimations of surface air temperature and of sea ice concentration, with the extremely efficient particle filter having the best performance. When reconstructing variables that are not directly linked to the pseudo-observations of surface air temperature as atmospheric circulation and sea surface salinity, the performance of the particle filters is weaker but still satisfactory for many applications. Sea surface salinity reconstructed by the nudging, however, exhibits a patterns opposite to the pseudo-observations, which is due to a spurious impact of the nudging on the ocean mixing.

1 Introduction

Reliable reconstructions of the past climate states are essential for a comprehensive understanding of the climate system, more accurate climate predictions and projections. They enable to estimate the magnitude of the natural variability without anthropogenic impact and to provide insights into the processes responsible for climate changes.

A new but highly appealing approach to reconstruct the past climate states is data assimilation, (e.g. Bhend et al., 2012; Widmann et al., 2010; Annan and Hargreaves,

CPD

9, 43–74, 2013

An assessment of climate state reconstructions

S. Dubinkina and
H. Goosse

Title Page

Abstract

Introduction

Conclusions

References

Tables

Figures

⏪

⏩

◀

▶

Back

Close

Full Screen / Esc

Printer-friendly Version

Interactive Discussion



An assessment of climate state reconstructions

S. Dubinkina and
H. Goosse

[Title Page](#)[Abstract](#)[Introduction](#)[Conclusions](#)[References](#)[Tables](#)[Figures](#)[⏪](#)[⏩](#)[◀](#)[▶](#)[Back](#)[Close](#)[Full Screen / Esc](#)[Printer-friendly Version](#)[Interactive Discussion](#)

2012). The main purpose of data assimilation is to estimate the state of a system as accurately as possible incorporating all the available information: numerical modelling of the behaviour of the system, observations, and uncertainties of the model and of the observations (Talagrand, 1997). When choosing a data-assimilation method, the application to which it is applied should be kept in mind. For example, in meteorological applications data-assimilation methods like 4DVar (e.g. Courtier et al., 1994) or the ensemble Kalman filter (Evensen, 1994) are employed. These methods, however successful, are biased in the sense that they assume the Gaussian prior distribution. But the prior distribution can take any form because the system is nonlinear.

There exists an ensemble-based data-assimilation method that does not make such an assumption. It is particle filtering. In particle filtering, the probability distribution function of the state is approximated by an ensemble of particles, where a particle (or ensemble member) is a full model state obtained by running a model. In order to have non-identical particles a perturbation is applied to initial conditions, for example. Then, each particle is propagated forward in time using the model. When the observation becomes available, the so-called importance weights are assigned to the particles based on how close to the observation they are. Small weights are given to particles far from the observation; large weights, to particles close to the observation. The ensemble mean, which is the best estimate of the state, is then a sum of the particles each multiplied by the corresponding weight.

Particle filtering has no assumption of gaussianity, uses a full nonlinear model to propagate the particles, but unfortunately, suffers from the “curse of dimensionality” (Snyder et al., 2008), meaning that for a high-dimensional system and an ensemble of small size it leads to large variances in the particles (ensemble members) and, consequently, to large variance in the corresponding importance weights with only a few of them being relatively large. After a few data-assimilation cycles the importance weight of a single particle becomes close to one, while the weights of the other particles become close to zero. Consequently, the ensemble that has collapsed to a single particle can no longer approximate the probability distribution function of the state. Therefore,

An assessment of climate state reconstructions

S. Dubinkina and
H. Goosse

[Title Page](#)[Abstract](#)[Introduction](#)[Conclusions](#)[References](#)[Tables](#)[Figures](#)[Back](#)[Close](#)[Full Screen / Esc](#)[Printer-friendly Version](#)[Interactive Discussion](#)

particle filtering has not yet been employed for operational geophysical problems. To overcome the limitation of degeneracy, a new particle filter has been introduced by van Leeuwen (2010), the extremely efficient particle filter. There, the particles are guided towards the observations during the model simulations inducing smaller variance in the particles weights. The extremely efficient particle filter has shown good performance for the Lorenz-63 and the Lorenz-95 models (van Leeuwen, 2010), and for the barotropic vorticity equation (van Leeuwen and Ades, 2013).

Paleoclimate applications are somewhat different than meteorological applications. The system is nonlinear and high-dimensional as well, but the observations are sparse and have large uncertainties. Moreover, the available observations allow reconstructions of only large-scaled features averaged over several months or even years rather than a few tenths of kilometres and six hours scales. Therefore, for a paleoclimate application the number of degrees of freedom of the system can be reduced by performing spatial and temporal averages without substantial loss of needed information. This allows the use of a particle filter even without the “guidance” of van Leeuwen (2010). For instance, Goosse et al. (2009) used a particle filter with 96 members and the dataset HADCRUT3 (Brohan et al., 2006) to reconstruct the past half-century climate state in the Southern Hemisphere. It was shown that variables like surface air temperature averaged over large domains, sea ice area in the southern ocean, and the southern annual mode are in agreement with the observations at an annual time scale. Annan and Hargreaves (2012) assessed reconstructions of annual mean temperature anomalies over the Northern Hemisphere for the past two millennia. The reconstructions were obtained using a particle filter with 100 members and limited pseudo-proxies of surface temperature. It was pointed out that annual temperature at the hemispheric scale is well reconstructed, even when only 50 pseudo-proxies are used, as to the regional scale the performance is poor giving negative skill for the spatial field in some regions.

While those applications were dealing with annual reconstructions at a large spatial scale, our goal is to test data-assimilation methods to reconstruct the climate state with

**An assessment of
climate state
reconstructions**S. Dubinkina and
H. Goosse

Title Page

Abstract

Introduction

Conclusions

References

Tables

Figures

⏪

⏩

◀

▶

Back

Close

Full Screen / Esc

Printer-friendly Version

Interactive Discussion



a more detailed spatial structure and on a seasonal time scale. Since the number of degrees of freedom is larger when estimating seasonal variability than when estimating annual variability and the extremely efficient particle filter of van Leeuwen (2010) was specifically developed to handle high-dimensional systems with many degrees of freedom, we test this data-assimilation method in our experiments. Moreover, we compare the extremely efficient particle filter to a particle filter with sequential importance resampling, which was used by Dubinkina et al. (2011), and to a nudging – a data-assimilation method widely used by general circulation models for initializing climate predictions (e.g. Keenlyside et al., 2008; Pohlmann et al., 2009; Swingedouw et al., 2013).

In our studies, we focus on the Southern Hemisphere as it is an interesting test case for the model dynamics, including potentially complex interactions with sea ice. We employ the climate model of intermediate complexity LOVECLIM, a coupled model with atmospheric, oceanic, and sea-ice components. As the period of interest we choose 150 yr from year 1850 until year 2000. In this period of time, the anthropogenic impact varies, which allows to assess the performance of a data-assimilation method under different magnitudes of the forcing. Moreover, the study over such period of time, which is rather short for a paleoclimatological application, gives the basis for future applications on longer time scales.

Experiments with pseudo-proxies are quite typical for paleoclimatological applications (e.g. Smerdon, 2012), as they give more freedom in estimating skill of a method used to obtain a climate state reconstruction. Therefore, we constrain the model by pseudo-observations instead of instrumental records. We use pseudo-observations of surface air temperature anomalies, since for the last centuries observations of surface air temperature (either instrumental or proxy reconstructions) appear to be the most disposable. We perform two series of experiments: using the pseudo-observations given at every grid cell over the assimilated domain and using the pseudo-observations given at the same locations as the dataset of instrumental surface temperature records HADCRUT3. With the latter series we aim to approach a more realistic setup for

An assessment of climate state reconstructions

S. Dubinkina and
H. Goosse

Title Page

Abstract

Introduction

Conclusions

References

Tables

Figures

⏪

⏩

◀

▶

Back

Close

Full Screen / Esc

Printer-friendly Version

Interactive Discussion



a paleoclimatological application but without leaving the twin-experiment framework. The design of our experiments is close to a real application of a data-assimilation method (e.g. Goosse et al., 2012) and, therefore, can be easily adapted for such an application.

The paper is organized as follows: In Sect. 2, we give a description of three data-assimilation methods that are used for the past climate state reconstructions: the sequential importance resampling filter, a nudging, and the extremely efficient particle filter. In Sect. 3, we describe the climate model LOVECLIM and the experimental setup. Results of the experiments using the dense net of the pseudo-observations are given in Sect. 4. In Sect. 5, the performance of a data-assimilation method is addressed when the sparse net of the pseudo-observations is employed. Finally, conclusions are given in Sect. 6.

2 Data assimilation methods

2.1 Particle filter with sequential importance resampling

If the discrete equation for estimating the state ψ of a model at a time t_n is a function f of the state ψ at a time t_{n-1}

$$\psi^n = f(\psi^{n-1}), \quad (1)$$

then its M realizations, called particles, obtained using different initial conditions determine an ensemble $\{\psi_i^n\}_{i=1}^M$ that represents the model probability density as following

$$\rho(\psi^n) = K^{-1} \sum_{i=1}^M \delta(\psi^n - \psi_i^n), \quad (2)$$

where δ is a kernel density and K is a normalization factor. (Hereinafter any normalization factor will be denoted by K .) If there is no information about the model state

a priori, any particle is equally likely. But given the observation d^n of the model state ψ^n Bayes theorem indicates that the posterior probability is following

$$\rho(\psi^n|d^n) = K^{-1} \rho(d^n|\psi^n) \rho(\psi^n). \quad (3)$$

5 After using the density (2) in the theorem (3), the posterior probability becomes

$$\rho(\psi^n|d^n) = \sum_{i=1}^M w_i^n \delta(\psi^n - \psi_i^n) \quad \text{with} \quad w_i^n = K^{-1} \rho(d^n|\psi_i^n).$$

The weights $\{w_i^n\}_{i=1}^M$ are computed assuming that the likelihood $\rho(d^n|\psi_i^n)$ is Gaussian

$$\rho(d^n|\psi_i^n) = K^{-1} \exp \left[-\frac{1}{2} (d^n - H(\psi_i^n))^T R^{-1} (d^n - H(\psi_i^n)) \right]. \quad (4)$$

10 Here H is the measurement operator that projects a model state ψ_i^n to the location of the observation d^n , and R is the error covariance of the observations.

The last step of the sequential importance resampling filter consists of particles resampling according to their weights, which is often necessary to avoid the filter degeneracy. The particles with small weights are eliminated; whereas the particles with large weights are kept. To retain the total number of the particles the remaining particles are duplicated and perturbed. Then, the particles are propagated forward in time by the model until the next observation is available. After that, the importance weights are computed again but using the new observation, and the whole procedure is repeated until the end of the period of interest. For a more detailed description of the sequential importance resampling filter we refer the reader to van Leeuwen (2009).

2.2 Nudging

Nudging consists of a term that is added to the prognostic model equation in order to pull the model state towards the observation (e.g. Hoke and Anthes, 1976). In a discrete

An assessment of climate state reconstructions

S. Dubinkina and
H. Goosse

Title Page

Abstract

Introduction

Conclusions

References

Tables

Figures

⏪

⏩

◀

▶

Back

Close

Full Screen / Esc

Printer-friendly Version

Interactive Discussion



An assessment of climate state reconstructions

S. Dubinkina and
H. Goosse

Title Page

Abstract

Introduction

Conclusions

References

Tables

Figures

⏪

⏩

◀

▶

Back

Close

Full Screen / Esc

Printer-friendly Version

Interactive Discussion



$$W_i^n = K^{-1} p(d^n | \psi_i^n) \prod_{r=m+1}^n \frac{p(\psi_i^r | \psi_i^{r-1})}{q(\psi_i^r | \psi_i^{r-1}, d^n)}. \quad (6)$$

Here, index m is related to a time t_m at which the observation d^m – the observation previous to d^n – is available. Therefore, when computing the product in Eq. (6), all the model states $\{\psi_i^m, \psi_i^{m+1}, \dots, \psi_i^n\}$ between the two consecutive observations d^m and d^n are taken into account. If the observations are as frequent as the model states then $m+1 = n$, otherwise $m+1 < n$. Note, that the division in the computation of the weights (Eq. 6) does not lead to singularity since the support of the proposal transition density $q(\psi_i^r | \psi_i^{r-1}, d^n)$ is equal or wider than the one of the transitional density $p(\psi_i^r | \psi_i^{r-1})$ due to the presence of the stochastic noise ξ^r in the model equation (5). For computing the weights we take $p(d^n | \psi_i^n)$ to be equal to Eq. (4), the transition density to be equal to

$$p(\psi_i^r | \psi_i^{r-1}) = K^{-1} \exp \left[-\frac{1}{2} (\psi_i^r - f(\psi_i^{r-1}))^T C^{-1} (\psi_i^r - f(\psi_i^{r-1})) \right],$$

and the proposal transition density to be equal to

$$q(\psi_i^r | \psi_i^{r-1}, d^n) = K^{-1} \exp \left[-\frac{1}{2} (\xi_i^r)^T \Sigma^{-1} \xi_i^r \right].$$

The model error covariances C and Σ for simplicity are taken to be equal.

Since the nudging does not guarantee small variance in the particles and, consequently, in the importance weights when many degrees of freedom are present, the extremely efficient particle filter can still become degenerative. Therefore, the model states are generally adjusted just before the calculation of the weights such that the weights do not differ substantially afterwards. We, however, leave out this part of “almost equal weights” since the number of degrees of freedom in our application is still quite small. For a comprehensive explanation of the extremely efficient particle filter the reader is referred to van Leeuwen (2010); van Leeuwen and Ades (2013).

3 Description of experimental setup

The three-dimensional Earth system model of intermediate complexity LOVECLIM1.2 (Goosse et al., 2010) used here consists of the atmospheric component ECBILT2 (Opsteegh et al., 1998), the oceanic component CLIO3 (Goosse and Fichefet, 1999), and the terrestrial vegetation module VECODE (Brovkin et al., 2002). The atmospheric model is a three level quasi-geostrophic model of horizontal resolution T21 that includes a radiative scheme and a parametrisations of the heat exchanges with the surface. The free-surface ocean model is an ocean general circulation model coupled to a sea-ice model with horizontal resolution of three by three degrees and 20 unevenly spaced vertical levels in the ocean. The vegetation module describes annual changes in vegetation cover taking into account trees, grass and deserts; its horizontal resolution matches the resolution of the atmospheric component.

In the experiments, we use pseudo-observations of surface air temperature, to which we add a Gaussian noise with standard deviation 0.5°C in order to mimic the instrumental error. When comparing the reconstructions with the pseudo-observations no noise, however, is applied to the pseudo-observations, meaning that the comparison is done with the truth.

To constrain the model by the particle filters (either with sequential importance resampling or the extremely efficient one), we use the pseudo-observations averaged on a seasonal scale. The seasonal scale is small enough to provide with detailed climate state reconstructions but large enough not to impose the issue of degeneracy of the particle filters. Moreover, we apply a spatial filter to the particles as in Dubinkina et al. (2011) before computing the importance weights in order to reduce the number of degrees of freedom.

In the nudging (either alone or as a part of the extremely efficient particle filter), we use the pseudo-observations of monthly mean surface air temperature, since the nudging does not degenerate and monthly averages are generally the smallest scales of observations in long-term applications. The nudging is performed over the global

An assessment of climate state reconstructions

S. Dubinkina and
H. Goosse

Title Page

Abstract

Introduction

Conclusions

References

Tables

Figures

⏪

⏩

◀

▶

Back

Close

Full Screen / Esc

Printer-friendly Version

Interactive Discussion



ocean by introducing a term into the computation of heat fluxes coming from the atmosphere to the ocean. The nudging parameter α is chosen such that the heat flux adjustment due to the nudging is not larger than 50 W m^{-2} . The stochastic error ξ^n is constructed as following: empirical orthogonal function (EOF) analysis of the model error is performed taking into account the instrumental surface temperature records HADCRUT3 (Brohan et al., 2006) over the last 150 yr. Then, the noise is a sum of the first ten modes each multiplied by a random coefficient, and this noise together with the nudging term is added to the equation of heat fluxes.

In all three data-assimilation methods we use 96 particles, which seems to be sufficient for representing the probability density and is computationally affordable. The error covariance of the observations R is computed using the instrumental error and the error of representativeness, as in Dubinkina et al. (2011), and the model error covariance C is simply assumed to be a diagonal matrix with 0.5°C^2 on the diagonal.

4 Assimilation of the dense pseudo-observations

In the following experiments, the pseudo-observations of surface air temperature are given at every grid cell. Since assimilation of the pseudo-observations over the whole globe leads to filter degeneracy and assimilation over a small domain does not take many pseudo-observations into account, we make a compromise by choosing an area covering the polar cap southward of 30°S .

We examine the reconstructions of surface air temperature averaged over two domains: the area southward of 30°S and the area southward of 66°S (the top and bottom panels of Fig. 1). Reasonable reconstructions of surface air temperature are obtained using either the sequential importance resampling filter (blue curve) or the extremely efficient particle filter (red curve) over both domains. For the area southward of 30°S shown in the top panel of Fig. 1, the correlations for the sequential importance resampling filter and for the extremely efficient particle filter are 0.95 and 0.98, respectively, and the root mean square (RMS) errors are 0.07°C and 0.05°C , respectively. The

An assessment of climate state reconstructions

S. Dubinkina and
H. Goosse

Title Page

Abstract

Introduction

Conclusions

References

Tables

Figures

⏪

⏩

◀

▶

Back

Close

Full Screen / Esc

Printer-friendly Version

Interactive Discussion



An assessment of climate state reconstructions

S. Dubinkina and
H. Goosse

Title Page

Abstract

Introduction

Conclusions

References

Tables

Figures

⏪

⏩

◀

▶

Back

Close

Full Screen / Esc

Printer-friendly Version

Interactive Discussion



nudging performs also very well for the area southward of 30°S (green curve in the top panel of Fig. 1) providing with correlation of 0.93 and the RMS error of 0.09°C . But for the area southward of 66°S shown in the bottom panel of Fig. 1, its performance is weaker: correlation is 0.64 and the RMS error is 0.43°C . Moreover, the variance of the reconstructed anomaly (green curve) is smaller than the variance of the pseudo-observations (grey curve). This is due to the fact that the ocean covers a small fraction of the surface southward of 66°S ; therefore, since the nudging is done over the ocean only, it has a weaker direct influence on this area and propagation of the signal from the ocean to the land is not strong enough to lead to high correlations.

For estimating the performance of a data-assimilation method for the ocean reconstruction we consider ocean heat content. Figure 2 illustrates that ocean heat content is not significantly altered by the sequential importance resampling filter. Therefore, the sequential importance resampling filter does not change the heat budget of the climate model. Since the same forcing is used for deriving the pseudo-observations and when performing the data-assimilation experiments, ocean heat content from the sequential importance resampling filter is parallel to the pseudo-observations reflecting the influence of different initial conditions during the whole period. The nudging, on the contrary, has a strong influence on ocean heat content. This is due to the way the nudging is implemented: it adjusts heat fluxes from the atmosphere to the ocean. Consequently, ocean temperature changes, so does ocean heat content. The extremely efficient particle filter obtains ocean heat content that lies between the one from the nudging and the one from the sequential importance resampling filter and appears to be the closest to the pseudo-observations. To address the robustness of this result, we perform four experiments using different initial conditions for each data-assimilation method and investigate the RMS errors between ocean heat content reconstructed by a data-assimilation method and the pseudo-observations. We obtain that the mean RMS error using the extremely efficient particle filter is 0.008, using the sequential importance resampling filter it is 0.014, and using the nudging it is 0.013. Therefore,

ocean heat content from the extremely efficient particle filter has the smallest mean RMS error.

Next, we investigate the skill of the assimilation methods in reconstructing spatial features. In order to do that, we compute first empirical orthogonal functions (EOFs) of the pseudo-observations and project the results of model simulations onto them. Then, the corresponding principal components (PCs) and the projections are compared by means of correlation. We perform four experiments using different initial conditions for every data-assimilation method. The EOFs are computed for winter period (from May until October) over the area southward of 60°S , as we are mainly interested in the regions that are ice covered or that are close to the ice edge, and over a 21-yr period, since it is long enough to capture the main features of the state by the EOFs and short enough to split one model run in several such periods. Therefore, we divide a 150-yr run in six 21-yr periods starting from year 1865 and ending in year 1990, skipping the first 15 yr to avoid the bias induced by the initial conditions. Performing the EOF analysis over six 21-yr periods from four different experiments gives twenty-four correlations for every data-assimilation method.

In Fig. 3, we plot mean correlations plus and minus one standard deviation for different variables and different data-assimilation methods. When reconstructing surface air temperature (st) or sea ice concentration (sic) all three methods perform rather well providing with high correlations, as shown in the left panel of Fig. 3. Even a free model run (without data assimilation) has positive correlations, which is due to the employment of the same forcing when deriving the pseudo-observations. The skill of the extremely efficient particle filter when reconstructing surface air temperature is only slightly higher than the skill of the sequential importance resampling filter, as it is seen in the left panel of Fig. 3. When reconstructing sea ice concentration, however, the extremely efficient particle filter shows evident improvement compared to the sequential importance resampling filter. Indeed, as the corrections of heat fluxes from the atmosphere to the ocean have a strong impact on sea ice concentration, the nudging and the extremely

An assessment of climate state reconstructions

S. Dubinkina and
H. Goosse

[Title Page](#)[Abstract](#)[Introduction](#)[Conclusions](#)[References](#)[Tables](#)[Figures](#)[Back](#)[Close](#)[Full Screen / Esc](#)[Printer-friendly Version](#)[Interactive Discussion](#)

efficient particle filter have the higher skills than the sequential importance resampling filter.

Changes in atmospheric circulation is an important characteristics of past climate variability (e.g. Lefebvre and Goosse, 2008; Yuan and Li, 2008). Pressure observations that can be used to constrain the model in order to get reliable estimations of atmospheric circulation are, however, very limited for paleoclimate applications. Therefore, we investigate the skill of the atmospheric circulation reconstructions when surface air temperature is assimilated. We perform the EOF analysis for geopotential height, the variable in LOVECLIM that represents atmospheric circulation. In the left panel of Fig. 3, we see that correlations for geopotential height (geopg) are overall positive but not significant. To address this issue, we perform experiments with assimilating the pseudo-observations over a smaller domain: the area southward of 60°S instead of the area southward of 30°S. In the right panel of Fig. 3, we see that correlations for geopotential height are higher when the assimilation domain is smaller. This is due to a smaller number of degrees of freedom when assimilating over a smaller domain, which means that the particle filters are still close to degeneracy.

To continue with assessment of the performance of a data-assimilation method when reconstructing the ocean state, we perform the EOF analysis of sea surface salinity (sss), whose variations play a crucial role in the changes in density and, consequently, in the oceanic circulation and the vertical stability of the water column (e.g. Martinson, 1990; Gordon, 1991). In the left panel of Fig. 3, we see that the extremely efficient particle filter and the sequential importance resampling filter provide with positive and rather good correlations, taken into account that sea surface salinity is not directly linked to assimilated surface air temperature. By contrast, sea surface salinity obtained by the nudging has always negative correlations with the pseudo-observations. In order to understand the reason why the pattern of sea surface salinity obtained by the nudging is opposite to the pseudo-observations, we perform the EOF analysis for ocean temperature at different depths. As it is seen in Fig. 4, the nudging adjusts ocean temperature near the surface but does not respect the dynamics of the ocean. In particular,

An assessment of climate state reconstructions

S. Dubinkina and
H. Goosse

Title Page

Abstract

Introduction

Conclusions

References

Tables

Figures

⏪

⏩

◀

▶

Back

Close

Full Screen / Esc

Printer-friendly Version

Interactive Discussion



the nudging term strongly modifies the mixing (not shown) leading to a wrong vertical ocean temperature profile and to wrong vertical salinity.

5 Assimilation of the sparse pseudo-observations

In the following experiments, we investigate the performance of the data-assimilation methods when the pseudo-observations are as sparse as the dataset HADCRUT3 of the instrumental surface temperature records over the last 150 yr (Brohan et al., 2006) by selecting the pseudo-observations at the same locations as the HADCRUT3 dataset. The resolution of these pseudo-observations changes in time: for example, for year 1850 around 10 pseudo-observations are located in the area southward of 60° S and for year 2000 it is about 80. The number of the sparse pseudo-observations in the area southward of 60° S is substantially smaller compared to the area southward of 30° S: 80 sparse pseudo-observations against 400 for year 2000, for example. Since we are interested in the climate state reconstruction over the area southward of 60° S and the number of the sparse pseudo-observations in this area is very small, the prior distribution has to be chosen such that it increases the relative importance of the sparse pseudo-observations located in the area 90° S–60° S compared to the sparse pseudo-observations located in the area 60° S–30° S or decrease the data-assimilation area. Here, we keep the prior distribution to be uniform but assimilate the sparse pseudo-observations over a smaller area: the area southward of 60° S. The nudging, however, is still applied over the global ocean.

In Fig. 5, we plot time series of surface air temperature anomalies averaged over the area southward of 30° S (the top panel) and over the area southward of 66° S (the bottom panel). Compared to the case of assimilating the dense dataset of the pseudo-observations, the variance of the anomalies is underestimated, which is due to the sparse net of the pseudo-observations. Annan and Hargreaves (2012) has also observed the decrease in the variance when the pseudo-observations become more sparse. Nevertheless, all three data-assimilation methods estimate still reasonably well

An assessment of climate state reconstructions

S. Dubinkina and
H. Goosse

Title Page

Abstract

Introduction

Conclusions

References

Tables

Figures



Back

Close

Full Screen / Esc

Printer-friendly Version

Interactive Discussion



pseudo-observations and projections of model simulations onto the corresponding first EOFs of the pseudo-observations. Mean and standard deviation are computed over five correlations.

Figure 7 illustrates that the extremely efficient particle filter provides overall with higher correlations than any other method when reconstructing surface air temperature. Compared to the case of assimilating the dense pseudo-observation dataset, assimilation of the sparse pseudo-observations results in smaller mean correlations and larger standard deviations, except for the period 1970–1990, at which many pseudo-observations are available.

In Fig. 8, we see that even for the end of the 19th century, when the pseudo-observations are very sparse, correlations given by the extremely efficient particle filter and by the sequential importance resampling filter are quite reasonable for sea ice concentration, unlike the correlations given by the nudging. Moreover, the extremely efficient particle filter reconstructs sea ice concentration better than the sequential importance resampling filter, like in the case of assimilating the dense pseudo-observations.

From Fig. 9 we see that the data-assimilation methods do not constrain the model well enough in order to have reliable estimations of atmospheric circulation. Only in the period 1970–1990 with many pseudo-observations, correlations improve and become comparable to the correlations for geopotential height when assimilating the dense pseudo-observation dataset over the area southward of 60° S (the right panel of Fig. 3).

When reconstructing sea surface salinity, which is shown in Fig. 10, the extremely efficient particle filter performs quite well together with the sequential importance resampling filter. Over some periods the extremely efficient particle filter gives higher correlations, over other periods it is the sequential importance resampling filter that provides with higher correlations. The nudging performs worse than any particle filter, and over some periods the sea surface salinity pattern obtained by the nudging is opposite to the pseudo-observations. This result is, however, less persistent when assimilating the sparse pseudo-observations than when assimilating the dense pseudo-observations, see Fig. 3.

An assessment of climate state reconstructions

S. Dubinkina and
H. Goosse

Title Page

Abstract

Introduction

Conclusions

References

Tables

Figures

⏪

⏩

◀

▶

Back

Close

Full Screen / Esc

Printer-friendly Version

Interactive Discussion



6 Conclusions

We have shown that the extremely efficient particle filter provides with quite encouraging results: global variables like ocean heat content and surface air temperature averaged over large domains are well estimated. When assimilating the dense pseudo-observation dataset, the extremely efficient particle filter provides with reasonable reconstructions of not only variables that are directly linked to the pseudo-observations of surface air temperature, as surface air temperature and sea ice concentration, but also variables as geopotential height and sea surface salinity. Reliable reconstructions of the latter variables are essential for paleoclimate applications since the observations of pressure and salinity are limited there. Moreover, these reconstructions give good perspectives for initializing climate predictions.

When assimilating the sparse pseudo-observations that are given at the same locations as the dataset of instrumental surface temperature records HADCRUT3, the performance of the extremely efficient particle filter is weaker due to the limited number of the pseudo-observations. Nevertheless, even at the end of the 19th century, the reconstructions of surface air temperature and of sea ice concentration are quite good. The reconstructions of geopotential height and of sea surface salinity display, however, a lower skill.

Overall, the extremely efficient particle filter achieves better or equivalent results compared to the sequential importance resampling filter. To be more precise, surface air temperature reconstructed by the sequential importance resampling filter has already high correlations with the pseudo-observations, and the extremely efficient particle filter introduces only a slight improvement. In reconstructing sea ice concentration, however, a clear improvement is accomplished by the extremely efficient particle filter compared to the sequential importance resampling filter. When it comes to the reconstruction of variables that are not directly linked to the pseudo-observations of surface air temperature as geopotential height and sea surface salinity, the performance of

CPD

9, 43–74, 2013

An assessment of climate state reconstructions

S. Dubinkina and
H. Goosse

Title Page

Abstract

Introduction

Conclusions

References

Tables

Figures

⏪

⏩

◀

▶

Back

Close

Full Screen / Esc

Printer-friendly Version

Interactive Discussion



the sequential importance resampling filter is equivalent to the performance of the extremely efficient particle filter.

Even though the nudging used here provides with good reconstructions of surface air temperature and of sea ice concentration, it has the drawback of not respecting the dynamics of the ocean, which results in the wrong vertical profile of ocean temperature and, consequently, in wrong pattern of sea surface salinity. Nudging of salinity and ocean temperature over the depth could be a possible solution to this problem, but it should be kept in mind that observations of deep ocean temperature and salinity are available only for the recent past.

The improvement brought by the extremely efficient particle filter is apparent, which makes a strong argument for the use of the extremely efficient particle filter in the climate state reconstruction. Some developments, however, are still needed in order to get reliable estimations of variables that are not strongly linked through the model dynamics to the assimilated surface air temperature such as geopotential height and salinity.

Acknowledgements. H. Goosse is Senior Research Associate with the F.R.S.-FNRS-Belgium. The research leading to these results has received funding from the F.R.S.-FNRS, the Belgian Federal Science Policy Office and the European Union's Seventh Framework programme (FP7/2007–2013) under grant agreement no. 243908, "Past4Future. Climate change – Learning from the past climate". This is Past4Future contribution no. X.

References

- Annan, J. D. and Hargreaves, J. C.: Identification of climatic state with limited proxy data, *Clim. Past*, 8, 1141–1151, doi:10.5194/cp-8-1141-2012, 2012. 44, 46, 57
- Bhend, J., Franke, J., Folini, D., Wild, M., and Brönnimann, S.: An ensemble-based approach to climate reconstructions, *Clim. Past*, 8, 963–976, doi:10.5194/cp-8-963-2012, 2012. 44
- Brohan, P., Kennedy, J., Harris, I., Tett, S., and Jones, P.: Uncertainty estimates in regional and global observed temperature changes: a new dataset from 1850, *J. Geophys. Res.*, 111, D12106, doi:10.1029/2005JD006548, 2006. 46, 53, 57

An assessment of climate state reconstructions

S. Dubinkina and
H. Goosse

Title Page

Abstract

Introduction

Conclusions

References

Tables

Figures



Back

Close

Full Screen / Esc

Printer-friendly Version

Interactive Discussion



An assessment of climate state reconstructions

S. Dubinkina and
H. Goosse

Title Page

Abstract

Introduction

Conclusions

References

Tables

Figures

⏪

⏩

◀

▶

Back

Close

Full Screen / Esc

Printer-friendly Version

Interactive Discussion



- Brovkin, V., Bendtsen, J., Claussen, M., Ganopolski, A., Kubatzki, C., Petoukhov, V., and Andreev, A.: Carbon cycle, vegetation and climate dynamics in the Holocene: experiments with the CLIMBER-2 model, *Global. Biogeochem. Cy.*, 16, 1139, doi:10.1029/2001GB001662, 2002. 52
- 5 Courtier, P., Thépaut, J.-N., and Hollingsworth, A.: A strategy for operational implementation of 4D-VAR, using an incremental approach, *Q. J. Roy. Meteor. Soc.*, 120, 1367–1387, doi:10.1002/qj.49712051912, 1994. 45
- Dubinkina, S., Goosse, H., Sallaz-Damaz, Y., Crespin, E., and Crucifix, M.: Testing a particle filter to reconstruct climate changes over the past centuries, *Int. J. Bifurcat. Chaos*, 21, 3611–3618, doi:10.1142/S0218127411030763, 2011. 47, 52, 53, 58
- 10 Evensen, G.: Sequential data assimilation with a nonlinear quasi-geostrophic model using Monte Carlo methods to forecast error statistics, *J. Geophys. Res.*, 99, 10143–10162, doi:10.1029/94JC00572, 1994. 45
- Goosse, H. and Fichefet, T.: Importance of ice-ocean interactions for the global ocean circulation: a model study, *J. Geophys. Res.*, 104, 23337–23355, 1999. 52
- Goosse, H., Lefebvre, W., de Montety, A., Crespin, E., and Orsi, A.: Consistent past half-century trends in the atmosphere, the sea ice and the ocean at high southern latitudes, *Clim. Dynam.*, 33, 999–1016, doi:10.1007/s00382-008-0500-9, 2009. 46
- Goosse, H., Brovkin, V., Fichefet, T., Haarsma, R., Huybrechts, P., Jongma, J., Mouchet, A., Selten, F., Barriat, P.-Y., Campin, J.-M., Deleersnijder, E., Driesschaert, E., Goelzer, H., Janssens, I., Loutre, M.-F., Morales Maqueda, M. A., Opsteegh, T., Mathieu, P.-P., Munhoven, G., Pettersson, E. J., Renssen, H., Roche, D. M., Schaeffer, M., Tartinville, B., Timmermann, A., and Weber, S. L.: Description of the Earth system model of intermediate complexity LOVECLIM version 1.2, *Geosci. Model Dev.*, 3, 603–633, doi:10.5194/gmd-3-603-2010, 2010. 52
- 20 25 Goosse, H., Crespin, E., Dubinkina, S., Loutre, M., Mann, M., Renssen, H., Sallaz-Damaz, Y., and Shindell, D.: The role of forcing and internal dynamics in explaining the “Medieval Climate Anomaly”, *Clim. Dynam.*, 39, 2847–2866, doi:10.1007/s00382-012-1297-0, 2012. 48
- Gordon, A.: Two Stable Modes of Southern Ocean Winter Stratification, in: *Deep Convection and Deep Water Formation in the Oceans Proceedings of the International Monterey Colloquium on Deep Convection and Deep Water Formation in the Oceans*, edited by: Chu, P. and Gascard, J., vol. 57 of Elsevier Oceanography Series, 17–35, Elsevier, Amsterdam, the Netherlands, doi:10.1016/S0422-9894(08)70058-8, 1991. 56
- 30

An assessment of climate state reconstructions

S. Dubinkina and
H. Goosse

Title Page

Abstract

Introduction

Conclusions

References

Tables

Figures

⏪

⏩

◀

▶

Back

Close

Full Screen / Esc

Printer-friendly Version

Interactive Discussion



- Hoke, J. and Anthes, R.: The initialization of numerical models by a dynamic relaxation technique, *Mon. Weather Rev.*, 104, 1551–1556, 1976. 49
- Keenlyside, N., Latif, M., Jungclaus, J., Kornblueh, L., and Roeckner, E.: Advancing decadal-scale climate prediction in the North Atlantic sector, *Nature*, 53, 84–88, doi:10.1038/nature06921, 2008. 47
- Lefebvre, W. and Goosse, H.: An analysis of the atmospheric processes driving the large-scale winter sea-ice variability in the Southern Ocean, *J. Geophys. Res.*, 113, C02004, doi:10.1029/2006JC004032, 2008. 56
- Martinson, D.: Evolution of the Southern Ocean winter mixed layer and sea ice: open ocean deepwater formation and ventilation, *J. Geophys. Res.*, 95, 11641–11654, doi:10.1029/JC095iC07p11641, 1990. 56
- Opsteegh, J., Haarsma, R., Selten, F., and Kattenberg, A.: ECBILT: A dynamic alternative to mixed boundary conditions in ocean models, *Tellus*, 50A, 348–367, doi:10.1034/j.1600-0870.1998.t01-1-00007.x, 1998. 52
- Pohlmann, H., Jungclaus, J., Köhl, A., Stammer, D., and Marotzke, J.: Initializing decadal climate predictions with the gecco oceanic synthesis: effects on the north atlantic, *J. Climate*, 22, 3926–3938, doi:10.1175/2009JCLI2535.1, 2009. 47
- Smerdon, J.: Climate models as a test bed for climate reconstruction methods: pseudoproxy experiments, *WIREs Clim. Change*, 3, 63–77, doi:10.1002/wcc.149, 2012. 47
- Snyder, C., Bengtsson, T., Bickel, P., and Anderson, J.: Obstacles to high-dimensional particle filtering, *Mon. Weather Rev.*, 136, 4629–4640, doi:10.1175/2008MWR2529.1, 2008. 45
- Swingedouw, D., Mignot, J., Labtoulle, S., Guilyardi, E., and Madec, G.: Initialisation and predictability of the AMOC over the last 50 years in a climate model, *Clim. Dynam.*, doi:10.1007/s00382-012-1516-8, in press, 2013. 47, 50
- Talagrand, O.: Assimilation of observations, an introduction, *J. Meteorol. Soc. JPN*, Special Issue 75, 191–209, 1997. 45
- van Leeuwen, P.: Particle Filtering in Geophysical Systems, *Mon. Weather Rev.*, 137, 4089–4114, doi:10.1175/2009MWR2835.1, 2009. 49
- van Leeuwen, P.: Nonlinear data assimilation in geosciences: an extremely efficient particle filter, *Q. J. Roy. Meteor. Soc.*, 136, 1991–1999, doi:10.1002/qj.699, 2010. 46, 47, 51
- van Leeuwen, P. and Ades, M.: Efficient fully nonlinear data assimilation for geophysical fluid dynamics, *Comput. Geosci.*, doi:10.1016/j.cageo.2012.04.015, in press, 2013. 46, 51

Widmann, M., Goosse, H., van der Schrier, G., Schnur, R., and Barkmeijer, J.: Using data assimilation to study extratropical Northern Hemisphere climate over the last millennium, *Clim. Past*, 6, 627–644, doi:10.5194/cp-6-627-2010, 2010. 44

5 Yuan, X. and Li, C.: Climate modes in southern high latitudes and their impact on Antarctic sea ice, *J. Geophys. Res.*, 113, C06S91, doi:10.1029/2006JC004067, 2008. 56

An assessment of climate state reconstructions

S. Dubinkina and
H. Goosse

Title Page

Abstract

Introduction

Conclusions

References

Tables

Figures



Back

Close

Full Screen / Esc

Printer-friendly Version

Interactive Discussion



An assessment of climate state reconstructions

S. Dubinkina and
H. Goosse

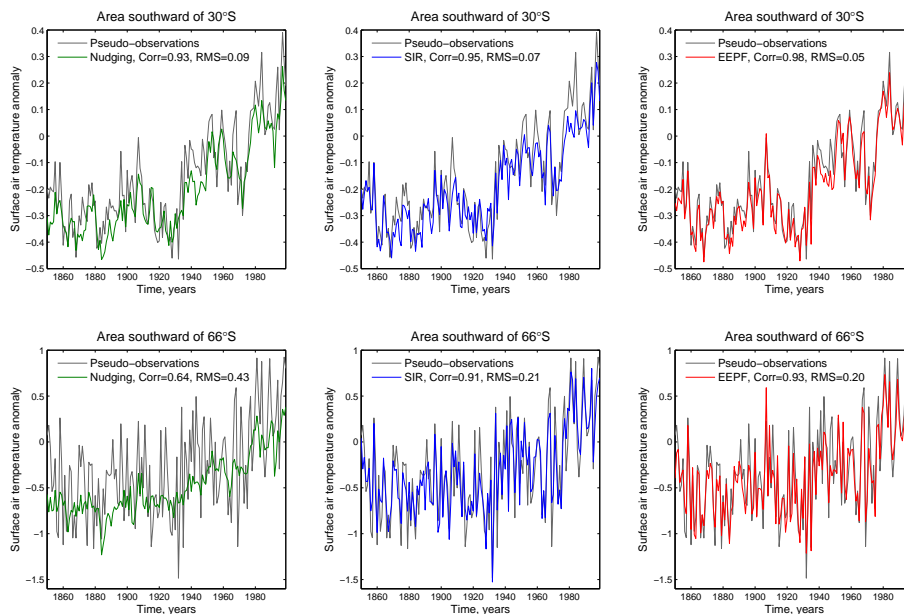


Fig. 1. Grey line: pseudo-observation of surface air temperature anomalies; green line: surface air temperature anomalies obtained using the nudging; blue line: surface air temperature anomalies obtained using the sequential importance resampling; red line: surface air temperature anomalies obtained using the extremely efficient particle filter. Correlations and the RMS errors are displayed in upper left corners. Top: average over the area southward of 30° S; Bottom: average over the area southward of 66° S.

Title Page

Abstract

Introduction

Conclusions

References

Tables

Figures

⏪

⏩

◀

▶

Back

Close

Full Screen / Esc

Printer-friendly Version

Interactive Discussion

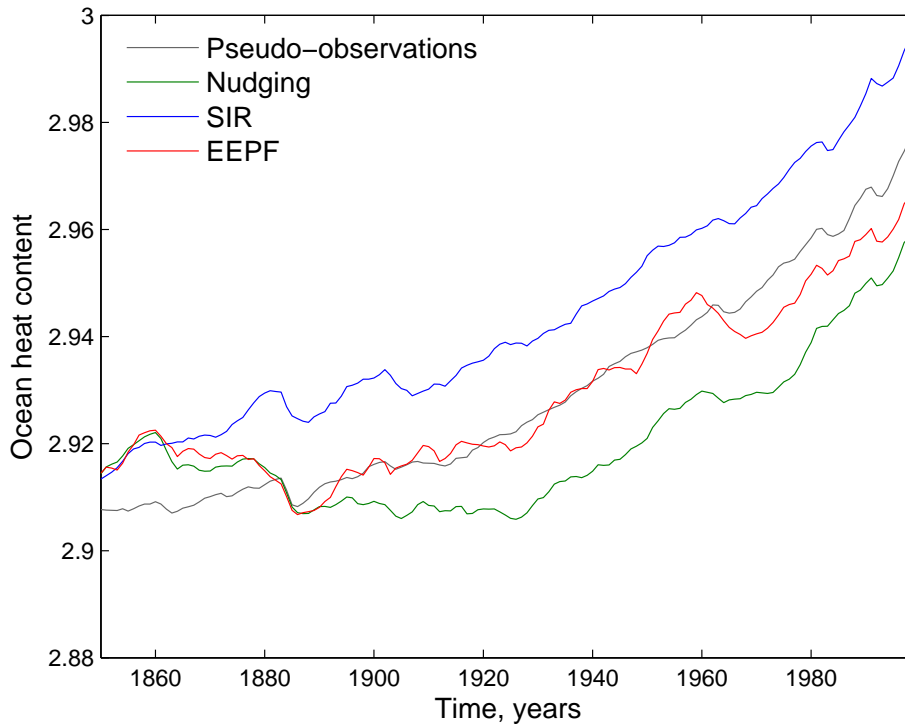


Fig. 2. Grey line: pseudo-observation of ocean heat content; green line: ocean heat content obtained using the nudging; blue line: ocean heat content obtained using the sequential importance resampling filter; red line: ocean heat content obtained using the extremely efficient particle filter.

An assessment of climate state reconstructions

S. Dubinkina and
H. Goosse

Title Page

Abstract

Introduction

Conclusions

References

Tables

Figures



Back

Close

Full Screen / Esc

Printer-friendly Version

Interactive Discussion



An assessment of climate state reconstructions

S. Dubinkina and
H. Goosse

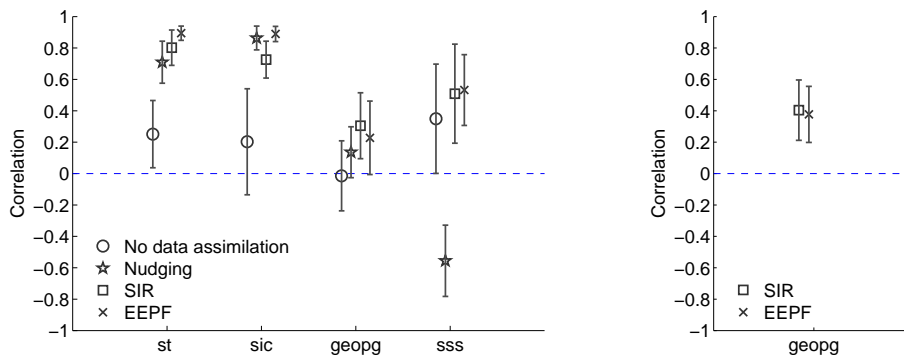


Fig. 3. Correlations between first PCs of the pseudo-observations and projections of the model simulations onto the corresponding first EOFs of the pseudo-observations for different variables: st is for surface temperature, sic is for sea ice concentration, geopg is for geopotential height, sss is for sea surface salinity. EOFs are computed for May–October of twenty-four 21-yr periods over the area southward of 60°S . The circle is the mean correlation for a free model run; the star is the mean correlation for the model simulations using the nudging; the square is the mean correlation for the model simulations using the sequential importance resampling filter; the cross is the mean correlation for the model simulations using the extremely efficient particle filter. Error bars correspond to one standard deviation. Left: the pseudo-observations are assimilated over the area southward of 30°S ; Right: the pseudo-observations are assimilated over the area southward of 60°S .

[Title Page](#)
[Abstract](#)
[Introduction](#)
[Conclusions](#)
[References](#)
[Tables](#)
[Figures](#)
[⏪](#)
[⏩](#)
[◀](#)
[▶](#)
[Back](#)
[Close](#)
[Full Screen / Esc](#)
[Printer-friendly Version](#)
[Interactive Discussion](#)

An assessment of climate state reconstructions

S. Dubinkina and
H. Goosse

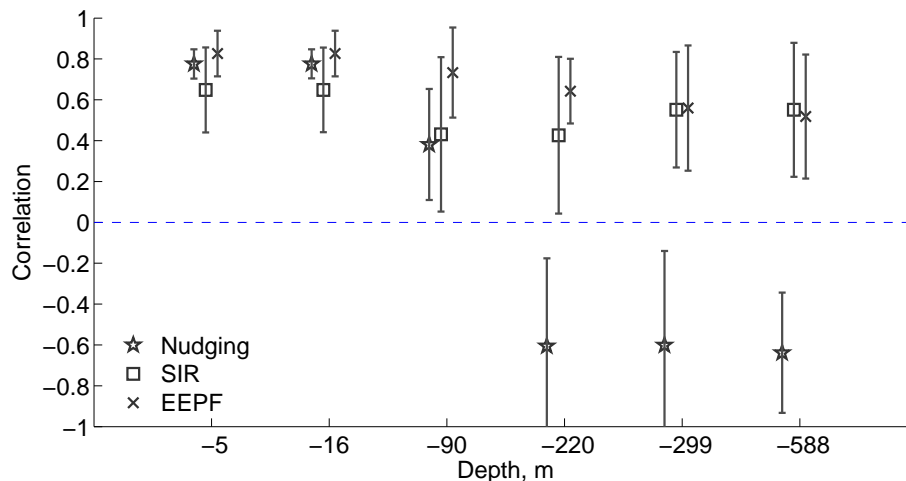


Fig. 4. Correlations between first PCs of the pseudo-observations and projections of the model simulations onto the corresponding first EOFs of the pseudo-observations for ocean temperature at different depths. EOFs are computed for May–October of six 21-yr periods over the area southward of 60° S. The star is the mean correlation for the model simulations using the nudging; the square is the mean correlation for the model simulations using the sequential importance resampling filter; the cross is the mean correlation for the model simulations using the extremely efficient particle filter. Error bars correspond to one standard deviation.

[Title Page](#)
[Abstract](#)
[Introduction](#)
[Conclusions](#)
[References](#)
[Tables](#)
[Figures](#)
[◀](#)
[▶](#)
[◀](#)
[▶](#)
[Back](#)
[Close](#)
[Full Screen / Esc](#)
[Printer-friendly Version](#)
[Interactive Discussion](#)

An assessment of climate state reconstructions

S. Dubinkina and
H. Goosse

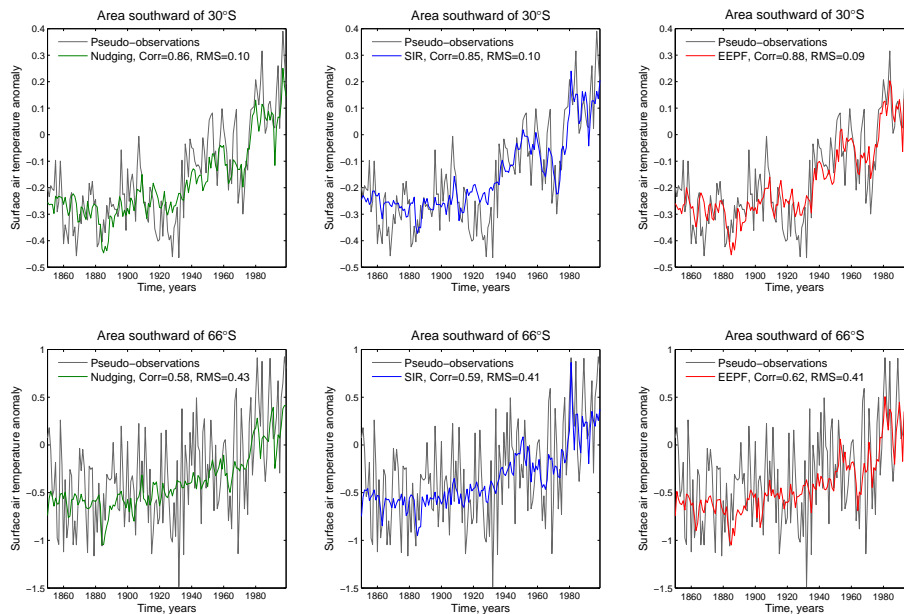


Fig. 5. Same as Fig. 1, but using the sparse pseudo-observations.

Title Page

Abstract

Introduction

Conclusions

References

Tables

Figures

◀

▶

◀

▶

Back

Close

Full Screen / Esc

Printer-friendly Version

Interactive Discussion

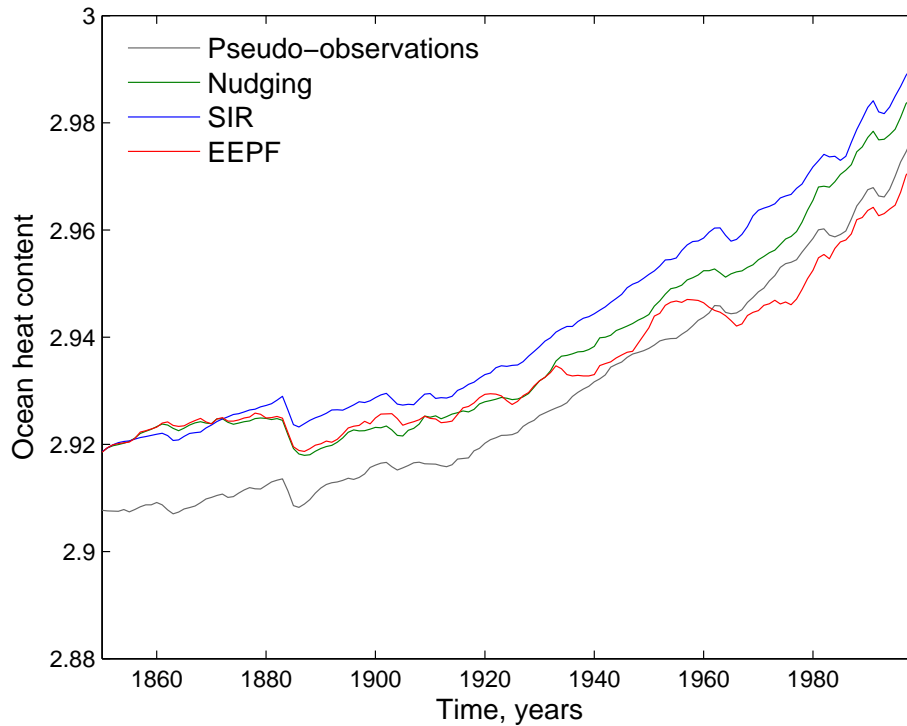


Fig. 6. Same as Fig. 2, but using the sparse pseudo-observations.

An assessment of climate state reconstructions

S. Dubinkina and H. Goosse

Title Page

Abstract Introduction

Conclusions References

Tables Figures

◀ ▶

◀ ▶

Back Close

Full Screen / Esc

Printer-friendly Version

Interactive Discussion



An assessment of climate state reconstructions

S. Dubinkina and
H. Goosse

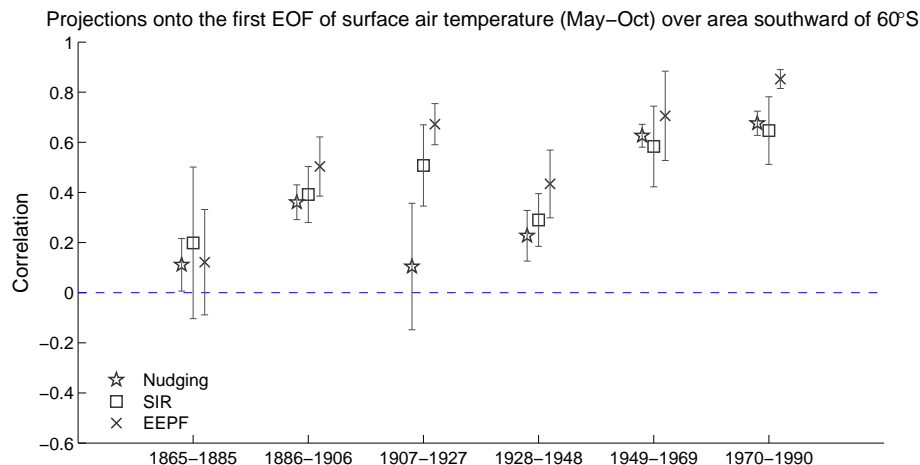


Fig. 7. Correlations between first PCs of the pseudo-observations and projections of model simulations onto the corresponding first EOFs of the pseudo-observations for surface air temperature for different time periods. EOFs are computed over the area southward of 60°S for May–October of 21-yr periods from five runs. The star is the mean correlation obtained using the nudging; the square is the mean correlation obtained using the sequential importance re-sampling filter; the cross is the mean correlation obtained using the extremely efficient particle filter. Error bars correspond to one standard deviation.

Title Page

Abstract

Introduction

Conclusions

References

Tables

Figures

⏪

⏩

◀

▶

Back

Close

Full Screen / Esc

Printer-friendly Version

Interactive Discussion

An assessment of climate state reconstructions

S. Dubinkina and
H. Goosse

Title Page

Abstract

Introduction

Conclusions

References

Tables

Figures

◀

▶

◀

▶

Back

Close

Full Screen / Esc

Printer-friendly Version

Interactive Discussion

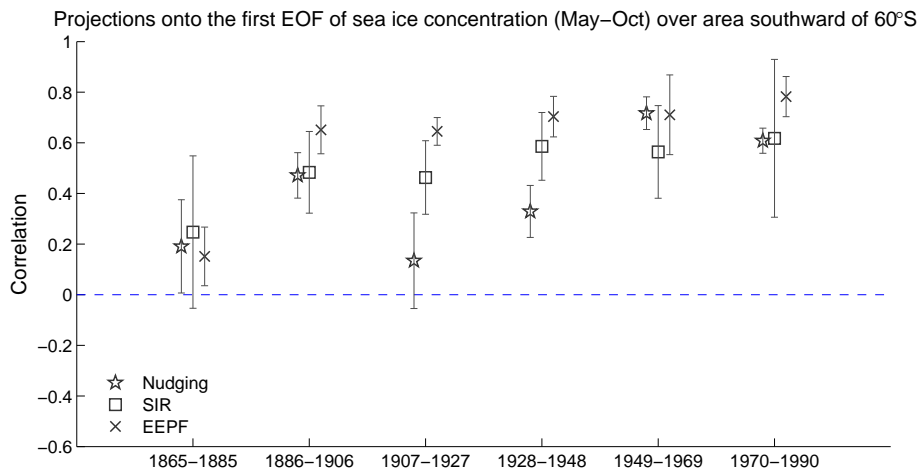


Fig. 8. Same as Fig. 7, but for sea ice concentration.

An assessment of climate state reconstructions

S. Dubinkina and
H. Goosse

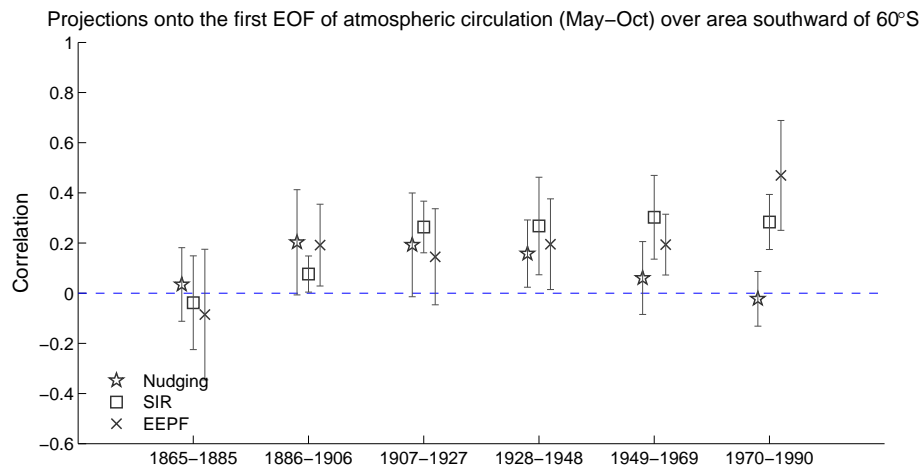


Fig. 9. Same as Fig. 7, but for geopotential height.

Title Page

Abstract

Introduction

Conclusions

References

Tables

Figures

◀

▶

◀

▶

Back

Close

Full Screen / Esc

Printer-friendly Version

Interactive Discussion

An assessment of climate state reconstructions

S. Dubinkina and
H. Goosse

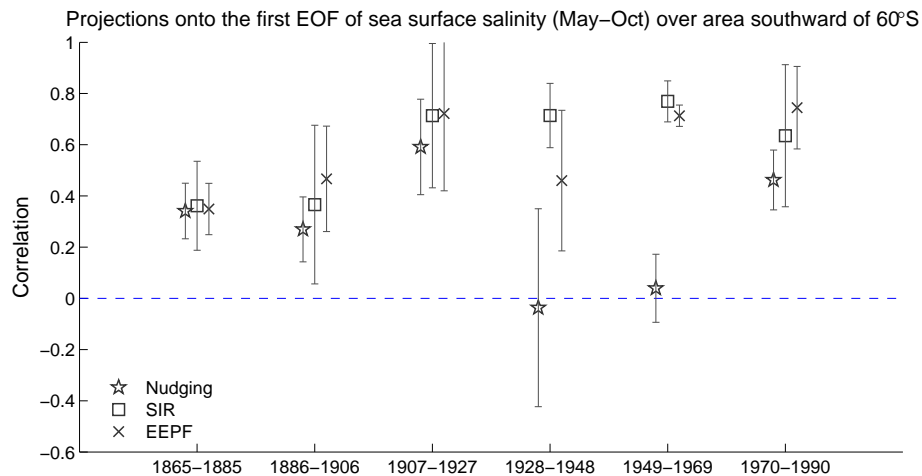


Fig. 10. Same as Fig. 7, but for sea surface salinity.

Title Page

Abstract

Introduction

Conclusions

References

Tables

Figures

⏪

⏩

◀

▶

Back

Close

Full Screen / Esc

Printer-friendly Version

Interactive Discussion